

Auger Electron Emission from Fixed-in-Space CO

Th. Weber,¹ M. Weckenbrock,¹ M. Balsler,¹ L. Schmidt,¹ O. Jagutzki,¹ W. Arnold,¹ O. Hohn,¹ M. Schöffler,¹ E. Arenholz,² T. Young,² T. Osipov,³ L. Foucar,^{1,2} A. De Fanis,⁴ R. Díez Muiño,⁵ H. Schmidt-Böcking,¹ C. L. Cocke,³ M. H. Prior,² and R. Dörner^{1,*}

¹*Institut für Kernphysik, University Frankfurt, August-Euler Strasse 6, D-60486 Frankfurt Germany*

²*Lawrence Berkeley National Laboratory, Berkeley, California 94720*

³*Department of Physics, Kansas State University, Cardwell Hall, Manhattan, Kansas 66506*

⁴*Institute of Multidisciplinary Research for Advanced Materials, Tohoku University, Sendai 980-8577, Japan*

⁵*Donostia International Physics Center DIPC, P. Manuel de Lardizabal 4, 20018 San Sebastián, Spain*

(Received 20 August 2002; published 16 April 2003)

We have measured the angular distribution of carbon *K*-Auger electrons from fixed in space, core-ionized, CO molecules in coincidence with the kinetic energy release of the C⁺ and O⁺ fragments. We find a very narrow ejection of Auger electrons in the direction of the oxygen and an oscillatory diffraction pattern. Even for similar electron energies, the angular distribution strongly depends on the symmetry of the final state.

DOI: 10.1103/PhysRevLett.90.153003

PACS numbers: 32.80.Hd, 33.20.-t, 33.80.-b

The study of Auger decay from molecules still pursues many open questions. One of the challenges results from the number and complexity of the final states. The many very broad overlapping structures in the Auger energy distribution often do not allow for a clear assignment of the decay channel [1]. A second challenge results from the interaction of the Auger electron with the molecular potential. Similar to photoelectrons [2,3] the Auger electron will be multiply scattered in the molecule hence modifying Auger rates and angular distributions. A third challenge was posed recently by the claim [4] that even off resonance the creation of a core hole by photoionization and its subsequent Auger decay cannot be treated as two independent steps (two-step model), as has been commonly assumed [2,5].

In the present Letter we address these three challenges by reporting an experiment on the Auger decay of carbon *K*-shell ionized CO⁺. We have measured the Auger electron energy and angle in coincidence with the energy and angle of both fragment ions of the CO²⁺. Such complete monitoring of the process results in a qualitatively new level of insight into the molecular Auger decay. First the high resolution in electron energy and kinetic energy release (KER) allows determination of the final electronic states of the C⁺ and O⁺ fragments which in turn helps to identify the molecular decay channel. Second and more importantly, the measurement of the direction of fragmentation often, *a posteriori*, determines the molecular axis at the instant of Auger emission. We therefore obtain Auger electron angular distributions in the molecular frame. These have, as we show below, a very rich structure. It has been emphasized from the theory side that the angular distributions from fixed-in-space molecules are a key to a deeper understanding of the molecular Auger process [2,6,7]. Zähringer *et al.* have shown that the Auger electron angular distribution can be understood as resulting from two processes acting together. The sym-

metry of the molecular states involved and their non-spherical electron density lead to a coarse structure. On top of this a diffraction pattern from the interaction of the Auger electron wave with the molecular potential has been seen in the calculations. None of these effects have been observed experimentally until now [4,8].

The experiment was performed at BL 4.0 [9] of the Advanced Light Source using the COLTRIMS technique (cold target recoil ion momentum spectroscopy) [10]. The photon beam intersected a supersonic molecular gas jet. The ionic fragments are collected by a static electric extraction field (15 V/cm) with 4 π solid angle acceptance and directed onto a 80 mm diameter position sensitive channel-plate detectors equipped with a delayline anode [11]. The electrons pass three regions of different homogenous electrical fields separated by meshes. The electron/ion extraction field of 15 V/cm over 2.9 cm is followed by a deceleration region of 4.4 cm with a final retarding voltage of -230 V with respect to the interaction point. The retarded electrons then drift over 11.5 cm before they reach an 80 mm diameter position sensitive channel-plate detector. A magnetic guiding field of 2.8 Gauss parallel to the electric fields yields an electron acceptance angle of 12 deg. With this deceleration scheme we achieve an energy resolution of <1 eV for electrons from 240–270 eV [see Fig. 2(b)]. This spectrometer combines the high energy resolution achieved by retarding the electrons with position sensitive detection which provides measurements at several angles at once. A series of measurements in which the polarization vector of the linearly polarized light was rotated in steps of 10 deg from parallel to perpendicular to the spectrometer axis [9] has been performed. We have verified the rotation of polarization by measuring the angular distribution of the C⁺ + O⁺ fragments [Fig. 1(a)]. The measurements for the different polarization directions have been normalized by the number of (C⁺ + O⁺) coincidences registered at each

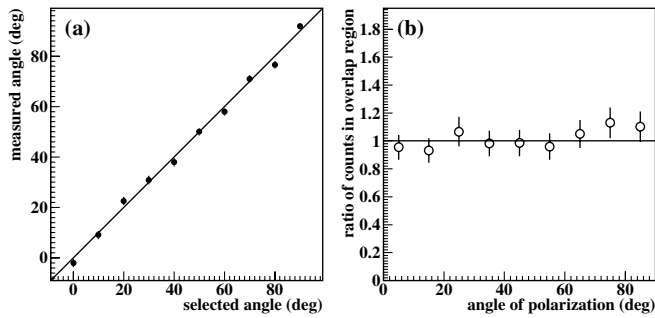


FIG. 1. (a) Cross check of rotation of polarization axis: Measured laboratory angle of the polarization axis obtained from fitting the experimental angular distribution of C^+O^+ fragmentation without detection of one electron as a function of the requested polarization angle for the undulator. (b) Cross check of our normalization procedure: ratio of normalized counts in the 9 electron detector overlapping region between neighboring settings of the the polarization axis angle (see text).

orientation of the polarization. Our Auger electron, C^+ , O^+ triple coincidence data are a subsample of these $C^+ + O^+$ double coincidence data, which are used for normalization. Therefore, this normalization procedure automatically accounts for all fluctuations of gas pressure, light flux, and data acquisition dead time. We have verified our normalization by the following completely independent method: Since our electron acceptance angle is 12 deg and the step size for the rotation of the polarization is 10 deg, there is a 2 deg overlap between the individual measurements. After normalizing our data sets we have compared the counts in the overlapping solid angle region between two neighboring measurements. Figure 1(b) shows the independence of the ratio of our normalized measurements in the overlapping regions with respect to the polarization angle. By the rotation of the polarization vector we collected a data set which covers all directions of the molecular axis and the Auger electron with respect to the polarization and to each other. In addition experiments for left and right circular polarized light have been performed.

The total energy available in the decay of the core-ionized CO^+ is shared between the Auger electron, the KER, and the internal electronic excitation energy in the ionic fragments. The correlation between Auger energy and kinetic energy release is shown in Fig. 2(a). Each of the final ionic states leads to a diagonal line (constant sum of KER and electron energy) in Fig. 2(a). The electronic ground state and the two first excited states are indicated by solid lines. The figure confirms earlier findings [1,12,14–16] that the narrow peak in the Auger spectrum at around 250.5 eV results from a decay to the second $1^1\Sigma^+$ potential curve [see the correlation diagram Fig. 2(c)] which then couples to the first $3^3\Sigma^-$ curve leading to the ionic ground states. This corresponds to a dominant peak at 10 eV in the KER spectrum [17,18]. Similarly the structure around 251–255 eV Auger energy corresponds

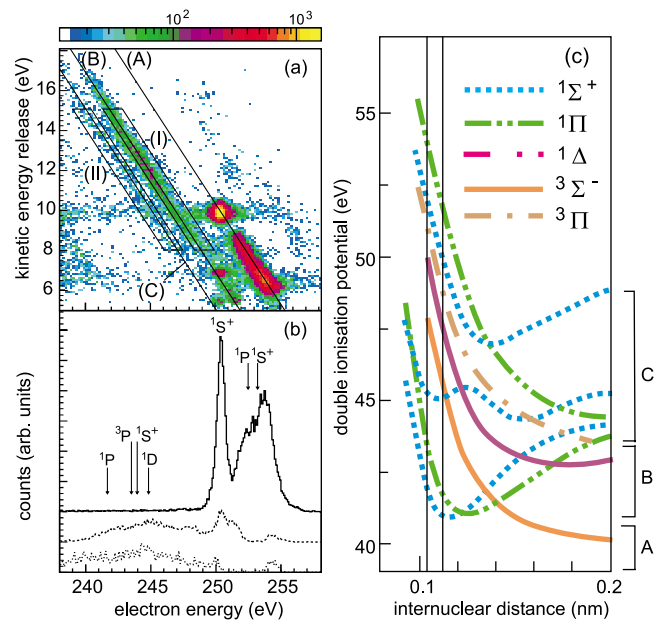


FIG. 2 (color online). Auger decay of CO^+ from 305 eV photon absorption leading to $C^+ + O^+$. (a) horizontal axis Auger electron energy, vertical axis kinetic energy release. The diagonal lines correspond to decays of the CO^+ [$C(1s)^{-1}$] ground state to different final states of the ionic fragments: (A): $C^+(^2P) + O^+(^4S)$ (ground state); (B): $C^+(^2P) + O^+(^2D)$; (C): $C^+(^2P) + O^+(^2P)$. (b) Auger electron spectra corresponding to (A), (B), and (C) final state (from top to bottom). The arrows show the calculated mean energies for some states from [12]. These calculated transitions have a width of 3–5 eV. The regions I and II are gates used for Fig. 4, see text. (c) Correlation diagram for CO^{2+} from [13]. For clarity only those states are shown which are discussed in the text. The Franck Condon region of $C(1s^{-1})$ is indicated by the vertical lines. The brackets on the right indicate the asymptotic ionic states as in (a). The asymptotic energies (at infinite internuclear distance) are 35.4, 38.7, and 40.4 eV for A, B, and C, respectively) (from [14]).

to a decay to the first $1^1\Pi$ and $1^1\Sigma^+$ state which finally decays to $C^+(^2P) + O^+(^2D)$.

Practically all KER above 10 eV yields fragment ions in the first two excited states of the O^+ ion [$O^+(^2D)$ and $O^+(^2P)$]. The calculations of Cederbaum *et al.* [12] and Schimmelpfennig and Peyerimhoff [16] allow an assignment of the dominant channels in this region. The area I in Fig. 2(a) has contributions from transition to $1^1\Pi$, $3^1\Pi$, and $1^1\Delta$ with a decay width of 0.83, 0.23, and 0.968 a.u. [16] (see also Fig. 2.). The only $1^1\Sigma^+$ state in this region decays exclusively to the $C^+(^2P) + O^+(^2P)$ final state (region II). In regions of the spectrum where several states overlap, the simultaneous measurement of KER and Auger energy thus allows separation of a channel containing electrons of only one symmetry. The additional weak features 3–6 eV to the right of line A results from the decay of excited CO^+ .

We now investigate the electron angular distributions for some of the decay paths. A particularly clean case is the narrow ${}^1\Sigma^+$ line (B state) at around 250.5 eV. For this line Guillemin *et al.* [4] have recently reported that, at a photon energy of 305 eV as used in our study, the angular distribution of the Auger electron depends on the direction of polarization of the photon which created the K hole. This would indicate a breakdown of the widely accepted independent two-step model (see, e.g., [2,5]). This model plausibly assumes that, if the Auger electron and photoelectron have very different energies, one can treat the first step of core level photoionization and the second one of core hole Auger decay as independent processes, i.e., that the Auger decay has no memory of how the K hole was produced. Our data are shown in Fig. 3 for linear polarized light with the polarization vector at 0, 45, and 90 deg to the molecular axis as well as for circularly polarized light. We do not observe the effect reported in [4]. Our Auger angular distributions are polarization independent and hence are consistent with the two-step model. Our measured distributions are only weakly structured. We argue that this is a consequence of the failure of the axial recoil approximation. In a previous study of the photoelectron angular distribution coincident with a KER of 10 eV [18], we have shown that the CO^{2+} for these decay channels lives long enough to rotate at least partially before fragmenting. In fact, the potential well in the second ${}^1\Sigma^+$ supports at least two vibrational states which can be seen in a high resolution KER spectrum [17,18].

We cannot definitely explain why the the results obtained in [4] diverge so strongly from our more complete measurements. However, we note that the reported retarding potential of 7 V in front of the ion detector used in [4] would not have allowed detection of the O^+ or C^+ fragments from the ${}^1\Sigma^+$ state since each has less than 6 eV kinetic energy.

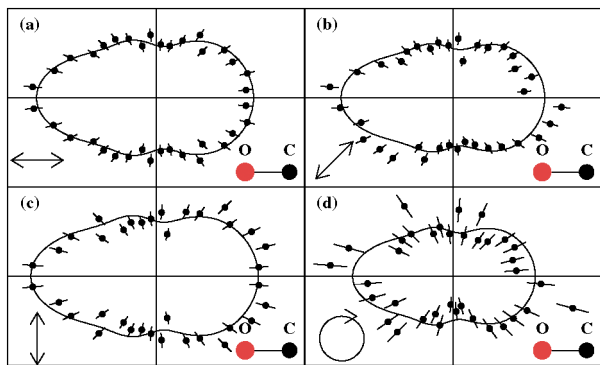


FIG. 3 (color online). Angular distribution of Auger electrons from the narrow ${}^1\Sigma^+$ line at 250.5 eV (B state) (see Fig. 2). The orientation of the molecule is horizontal with the oxygen to the left as indicated. (a)–(c) Linear polarized light, the polarization vector is indicated by the double arrow. (d) Circularly polarized light, propagating into the plane of the figure.

We have also investigated the angular distribution of electrons in the region between 251 and 255 eV which corresponds to the transition to the first ${}^1\Pi$ and ${}^1\Sigma^+$ state. They are referred to as \tilde{X} and \tilde{A} states in [4]. This angular distribution, not shown here because of limited space, is also completely polarization independent. Since also here the CO^+ ion is known to rotate before decay [18] the angular distribution is almost without structure. This distribution is in agreement with the corresponding data in [4].

Figure 4 shows the Auger electron angular distributions for the regions I and II in Fig. 2(a). For this high KER the axial recoil approximation is known to be valid [18]. The transition to the ${}^1\Pi$, ${}^3\Pi$, and ${}^1\Delta$ in region I shows an emission mainly perpendicular to the molecular axis, as one expects for a Π wave. The intensity is significantly shifted to the direction of the oxygen center.

A completely different pattern is found in Figs. 4(b) and 4(c) for the transition to the third ${}^1\Sigma^+$ state, located along line C region II in Fig. 2(a). It shows a very narrow peaked emission of the electrons along the molecular axis in the direction of the oxygen [Figs. 4(b) and 4(c)]. Such emission into the direction of the neighboring atom is known from photoelectron diffraction as “forward focusing” [19]. The screened Coulomb potential next to the source of a photoelectron wave can act as a lens which collects a large amount of the electron flux into the forward direction. In order for such a strong focusing to

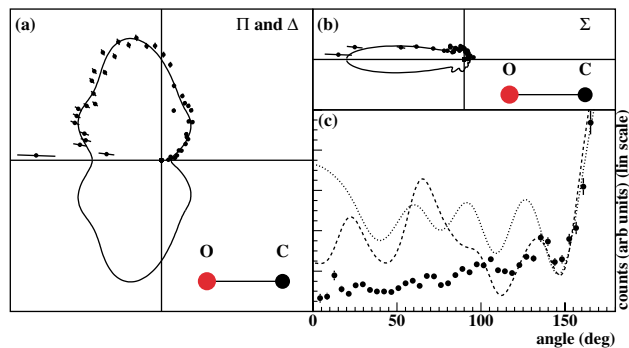


FIG. 4 (color online). Angular distribution of Auger electrons from CO^+ . (a) From region I, Fig. 2(a); (b) region II, Fig. 2(a). (a) corresponds to the $\text{CO}^+({}^1\Sigma^+) \rightarrow \text{CO}^{2+}({}^1\Delta, {}^3\Pi, {}^1\Pi)$ transition. (b) corresponds to a $\text{CO}^+({}^1\Sigma^+) \rightarrow \text{CO}^{2+}({}^1\Sigma)$ transition. (c) same data as in (b), 0 deg corresponds to emission in direction of the carbon. The full lines in all figures are a fit of Legendre polynomials to guide the eye. Other lines in (c) are results of a multiple scattering calculation for an S electron wave starting at the carbon center in CO^{2+} . Dashed: both vacancies in the CO^{2+} at $C(2p)$, dotted: one vacancy each at $C(2p)$ and $O(2p)$. The absolute height of the calculation is arbitrary. In all panels the cross section per solid angle $d\omega = d\vartheta d\phi$ is shown. It is obtained by dividing the raw data, which are for our 4π spectrometer per polar angle $d\vartheta$ by $\sin(\vartheta)$. The error bars in all panels show the statistical error. Where no error bars are visible they are smaller than the symbol size.

happen, the electron wave must have emerged from a localized region close to the carbon nucleus. This results from the Coulomb matrix element operating on an initial electron density distribution which has significant presence near the carbon core.

Inspection of this pattern [Fig. 4(c)] shows an oscillatory structure that is due to diffraction of the Auger electron wave in the two center potential as has been reported in the theoretical study of Zaehring [6]. To support this interpretation we have performed a multiple scattering calculation using spherical potentials (see [20] for calculational details). In this model we have launched an S wave from the carbon center in the CO^{2+} potential. In one model calculation we have located both CO^{2+} vacancies in a $2p$ orbital of the carbon center; in a second calculation, one vacancy at carbon $2p$ and one at oxygen $2p$. The position of the minima and maxima in both cases roughly coincides with the observed structure. Clearly this is not an appropriate model to describe the Auger decay; it serves only the heuristic purpose of identifying the physical origin of the observed oscillatory pattern.

In conclusion, our measurements provide a new level of insight into the molecular Auger decay. These electrons are emitted highly anisotropically. An extremely narrow jet of electrons along the molecular axis is found for a Σ transition. The symmetry of the transition is reflected in the angular distribution and a fine structure of electron diffraction is observed. Our experimental rehabilitation of the two-step model, previously questioned, reopens the road to a theoretical treatment of the molecular Auger decay with standard, non-time-dependent techniques.

This work was supported in part by DFG, BMBF, Chemical Sciences, Geosciences and Biosciences Division, Office of Basic Energy Sciences, Office of Science, U.S. Department of Energy. Th.W. thanks Graduiertenförderung des Landes Hessen for financial support. We thank Roentdek GmbH for support with the delayline detectors. We thank R. Guillemin and E. Shigemasa for motivating this study and V. Schmidt and T. Kerkau for helpful discussions.

*Electronic address: doerner@hsb.uni-frankfurt.de

[1] W.E. Moddeman, T. Carlson, M. Krause, B. Pullen, W. Bull, and G. Schweitz, *J. Chem. Phys.* **55**, 2317 (1971).

- [2] D. Dill, J.R. Swanson, S. Wallace, and J.L. Dehmer, *Phys. Rev. Lett.* **45**, 1393 (1980).
- [3] A. Landers, Th. Weber, I. Ali, A. Cassimi, M. Hattass, O. Jagutzki, A. Nauert, T. Osipov, A. Staudte, M.H. Prior, H. Schmidt-Böcking, C.L. Cocke, and R. Dörner, *Phys. Rev. Lett.* **87**, 013002 (2001).
- [4] R. Guillemin, E. Shigemasa, K.L. Guen, D. Ceolin, C. Miron, N. Leclercq, P. Morin, and M. Simon, *Phys. Rev. Lett.* **87**, 203001 (2001).
- [5] V.V. Kuznetsov and N.A. Cherepkov, *J. Electron Spectrosc. Relat. Phenom.* **79**, 437 (1996).
- [6] K. Zähringer, H.-D. Meyer, and L. Cerderbaum, *Phys. Rev. A* **46**, 5643 (1992).
- [7] S. Bonhoff, K. Bonhoff, and K. Blum, *J. Phys. B* **32**, 1139 (1999).
- [8] A. Edwards, Q. Zeng, R. Wood, and M. Mangan, *Phys. Rev. A* **55**, 4269 (1997).
- [9] A.T. Young, J. Feng, E. Arenholz, H.A. Padmore, T. Henderson, S. Marks, E. Hoyer, R. Schlueter, J.B. Kortright, V. Martynov, C. Steier, and G. Portmann, *Nucl. Instrum. Methods Phys. Res., Sect. A* **467**, 548 (2001).
- [10] R. Dörner, V. Mergel, O. Jagutzki, L. Spielberger, J. Ullrich, R. Moshhammer, and H. Schmidt-Böcking, *Phys. Rep.* **330**, 96 (2000).
- [11] (See <http://www.roentdek.com/> for details of the detectors.)
- [12] L. Cederbaum, P. Campos, F. Tarantelli, and A. Sgamellotti, *J. Chem. Phys.* **95**, 6634 (1991).
- [13] P. Lablanquie, J. Delwiche, M.-J. Hubin-Franskin, I. Nenner, P. Morin, K. Ito, J.H.D. Eland, J.-M. Robbe, G. Gandara, J. Fournier, and P.G. Fournier, *Phys. Rev. A* **40**, 5673 (1989).
- [14] T. Kerkau, dissertation, University Freiburg, Germany, 2000.
- [15] T. Kerkau and V. Schmidt, *J. Phys. B* **34**, 839 (2001).
- [16] B. Schimmelpfennig and S. Peyrimhoff, *Chem. Phys. Lett.* **253**, 377 (1996).
- [17] M. Lundqvist, P. Baltzer, D. Edvardsson, L. Karlsson, and B. Wannberg, *Phys. Rev. Lett.* **75**, 1058 (1995).
- [18] Th. Weber, O. Jagutzki, M. Hattass, A. Staudte, A. Nauert, L. Schmidt, M.H. Prior, A.L. Landers, A. Bräuning-Demian, H. Bräuning, C.L. Cocke, T. Osipov, I. Ali, R. Díez Muiño, D. Rolles, F.J. García de Abajo, C.S. Fadley, M.A. Van Hove, A. Cassimi, H. Schmidt-Böcking, and R. Dörner, *J. Phys. B* **34**, 3669 (2001).
- [19] H.C. Poon and S.Y. Tong, *Phys. Rev. B* **30**, 6211 (1984).
- [20] R.D. Muiño, D. Rolles, F.J.G. de Abajo, C.S. Fadley, and M.A.V. Hove, *J. Phys. B* **35**, L359 (2002).